Hydrochemistry and Nitrate Pollution of Groundwater in the Alluvial Aquifer of the Eastern Mitidja (Algeria)

Yamina SAYEH [1,2,a)], Ahcène SEMAR [2,3,b)] and Hakim BACHIR[4,c)]

[1] *Department of Rural Engineering, National High School of Agronomy (ENSA), Algiers, Algeria.*
[2] *Agricultural Water Management Laboratory, National High School of Agronomy (ENSA), Algiers, Algeria.*
[3] *Applied Geology Laboratory, Department of Soil Science, National High School of Agronomy (ENSA), Algiers, Algeria.*
[4] *National Institute for Agronomic Research, Algeria (INRAA), Algiers, Algeria .*

[a)] *hbb.sayeh@gmail.com*
[b)] *ahcene_semar@yahoo.fr*
[c)] *Corresponding Author akm7.62@hotmail.fr*

Abstract. The study carried out in the eastern Mitidja (Algeria) using groundwater chemistry data is aimed at clarifying the geochemical behavior of the alluvial groundwater as well as assessing the degree of nitrate contamination. The aquifer is characterized by a heterogeneous lithology marked by alternating levels of alluvium, gravel, sand and clay. The chemical facies encountered are: Na - Cl type with 52.7%, Mixed Ca - Mg - Cl type with 29.1%, Mixed Ca - Na - HCO$_3$ type with 9.1% and Ca – HCO$_3$ type with 9.1%. The interpretation of the analytical data shows that water mineralization is controlled by many ions Na+, SO42-, Cl-, Ca2+ and HCO3-. The Gibbs diagram suggests that weathering rock is the determining factor in the current chemical composition of groundwater. Agricultural activity is the main source of groundwater contamination by nitrates. Most of the water points tested have NO3 values very close to the critical threshold of 50 mg/l, the world health organization (WHO) drinking water reference value. By comparing this with the "human affected value" of 13 mg/l, 95% of the analyzed waters are considered contaminated. This water degradation is linked to the widespread use of nitrogen fertilizers, agricultural practices and increasing urbanization.

Keywords. Alluvial aquifer, Groundwater, Hydrochemistry, Nitrate pollution, Eastern Mitidja, Algeria.

I. INTRODUCTION

One of the most serious global environmental problems is groundwater pollution. Groundwater deterioration and pollution are region-specific [1]. The assessment and identification of groundwater mineralisation acquisition processes is an essential step in water resources management. Many scientific studies on the hydrochemical status of groundwater are conducted [2-8]. Other works have raised the importance and severity of nitrate pollution of groundwater [9-12]. This pollution can come from several sources, including atmospheric deposition, fauna and flora, mineralisation of organic matter, sewer and septic tank leakage, synthetic and organic agricultural fertilisers, leaching, infiltration of effluents, industrial contamination and other land uses. This work demonstrates the value of this resource for drinking water supply, irrigation and industry. The eastern plain of the Mitidja, considered as agricultural area, has become increasingly urbanised and industrialised [13]. Indeed, the increase in population combined with the development of the industrial framework means that this territory is being eroded year after year for infrastructure needs and consequently the agricultural sector is being impoverished. The Mitidja benefits from a rather favourable Mediterranean climate [14]. The relatively large and renewable water resource of the plain is heavily used to meet the needs of irrigation, the drinking water demand of part of the population and finally the needs of the industrial sector [15] . The alluvial aquifer of the Mitidja in northern Algeria is an important source of drinking, industrial and agricultural water. Unfortunately, nitrate contamination has led to a decline in water quality in several regions that benefit from this source [16]. Several studies have focused on the endemic nitrate pollution of groundwater in the Mitidja [17- 20]. Our work is also interested in this type of pollution. On the other hand, and in addition to the other works, the present study has two complementary objectives. The first part is a geochemical assessment of groundwater and the second part deals with nitrate contamination affecting the groundwater resource of the Eastern Mitidja.

II. STUDY AREA PRESENTATION

Situated in the North of Algeria, the study area is located in the eastern part of the Mitidja plain. With an area of about 80 km[2,] It stands between 547 781 m to 559 629 m longitudes East and 377 866.3 m to 387 184.1 m latitudes North. It is an integral part of the Mitidja plain known for it's agricultural vocation. The study area is bounded to the north by the Mediterranean Sea, to the west by the urban agglomerations of Bordj El Bahri and Bordj El Kiffan, to the south by Hammadi Street and to the east by Reghaia town. It is crossed by the Reghaia wadi, which originates in the southern hills (fig. 1.a). The soils are dominated by sandy silt texture. The Mitidja plain is an intra-mountainous basin, oriented ENE – WSW [21]. To the north, the plain is bounded by the Sahel plio-quaternary anticline whose contact is highlighted by a rift [22]. Quaternary formations are very heterogeneous; their granulometry varies in both vertical and horizontal directions [23]. They are characterized from bottom to top by coarse sediments that settle, in most of the plain, on the marls of El Harrach. The outcrops are located at the Sahel Anticline and in the eastern Mitidja (Reghaia region) where they constitute the eastern boundary of the basin. About, hydrogeological formation, two aquifers are recognized and exploited: the quaternary alluviums and the sandstone or calcareous sandstone reservoir of the Astian. The descriptions of these aquifers will focus mainly on the eastern part of the Mitidja. The groundwater is supplied by rainfall, from the wadis and by leakage from the Astian reservoir; it flows from south to north, the sea being its natural outlet. The groundwater is unconfined with a hydraulic continuity between the quaternary alluviums and the formation of the Astian (Fig. 1b). In the Rouiba region, transmissivity reaches $4*10^{-2}$ m^2/s and the storage coefficient varies from 3 to 10% . This aquifer is in contact with alluviums in the eastern part of the Mitidja. The general water flow is similar to that of alluvial deposits. In the Atlas, the quaternary aquifer feeds the Astian, while in the lower plain of El Harrach, alluviums are fed by the deep aquifer [24].
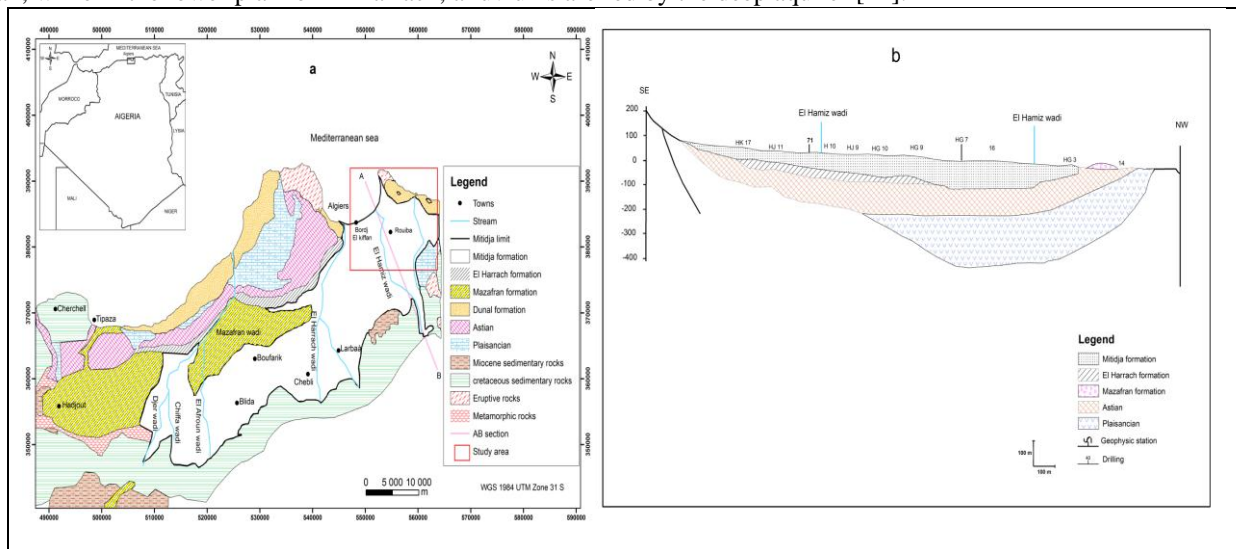

FIGURE 1. (a) Geological map of the Mitidja plain and (b) geological cross-section according to Bennie & Partners (1983).

The climate of the Mitidja plain is Mediterranean with hot and dry summers and mild and humid winters. The proximity of the Mediterranean Sea influences climatic parameters, in particular precipitation and humidity [25, 26]. Proximity to the Mediterranean Sea and presence of relief often give rise to both deep and shallow convection events.

III. METHODOLOGY

- **Water Sampling and Analysis**

Water points are boreholes and wells used for crop irrigation. This network is chosen according to a spatial hierarchy in terms of the availability of agricultural boreholes, in order to have a better representation of the area. Water sampling focused on groundwater in the alluvial aquifer of the eastern Mitidja. The sampling campaign took place from 25 to 30 October 2017, where 55 samples (10 wells and 45 boreholes) were collected through boreholes and artisanal wells as represented in fig.2.
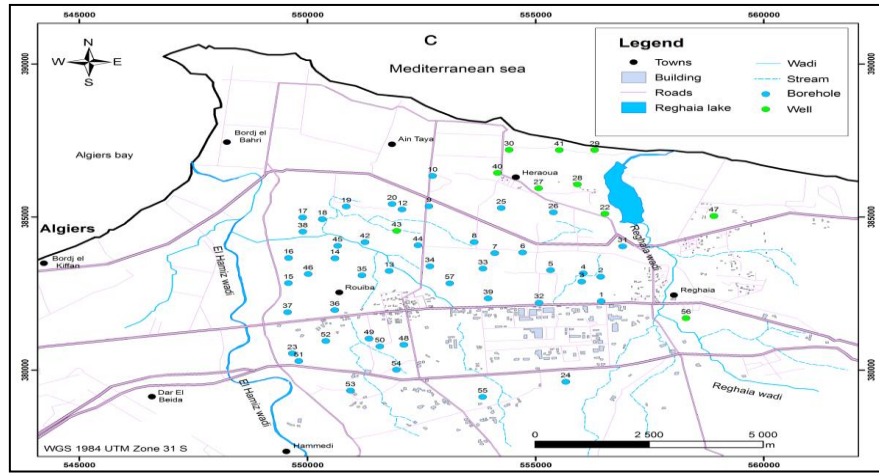
FIGURE 2. Sampling localization .

The collected samples are acidified with sulphuric acid $H_2SO_4^{2-}$ at pH =2. Field measurements (pH and T) are performed by a pH/EC/TDS/T° Tester, the EC is determined by means of a field conductivity meter. Calcium, sodium and potassium are evaluated by flame photometry while the total hardness is determined by the titrimetry method with respect to the EDTA standard solution [27], magnesium is deduced. Bicarbonates are determined by the titrimetric method in the presence of methyl orange. However chloride concentrations are determined by a ionometer. Nitrate and phosphorus contents are determined by UV spectrophotometry and sulphates by conductivity method. The quality of the hydrochemical data is assessed by the ion balance establishing the relationship between all cations (Ca^{2+}, Mg^{2+}, Na^+, K^+) and the total anions (Cl^-, SO_4^{2-}, HCO_3^-, NO_3^- and PO_4^{3-}) for each complete analysis. Validation of analytical results is based on error calculation and a threshold of 10% is tolerated [28].

- **Hydrochemistry Analysis**

Some indicators and indices were used to represent hydrochimical characteristic such as Saturation index, chloro Alkaline index, Gibbs diagram. The representation of chemical facies makes it possible to identify the order of cations and dominant anions present in water. We opted for the Piper diagram because it allows us to project several water points, compare them and determine any groups formed and monitor their evolution, especially when mineralization increases. This diagram is produced using the Diagrams software [29] which is composed of two triangles, allowing to represent the cationic and anionic facies, and a diamond synthesizing the global facies.

The saturation index is an essential parameter in hydrogeological and geochemical studies because it makes it possible to identify the behaviour of certain key minerals in groundwater. In this study, the saturation indices used are those for calcite, dolomite, aragonite, gypsum, anhydrite and halite. The saturation index is calculated according to relationship 1.

$$SI = Log\ IAP/K_T \qquad (1)$$

Where IAP is ion activity product and K_T is the equilibrium constant of the reaction considered at the sample temperature (SI is saturation index of a mineral, IAP = ion activity product of the dissociated mineral, KT = equilibrium solubility at mineral temperature). The geochemical code Phreeqc (Parkhurst and Appelo, 2013) is used to evaluate saturation indices. When groundwater is saturated with minerals, the SI values are zero; for positive SI values, the state is oversaturated, and for negative values, it indicates under-saturated [30,31]. Schoeller [32]. proposed chloroalkaline indices to highlight cation exchanges between groundwater and the solid matrix of the hydrogeological reservoir. These indices are widely used in hydrochemistry to identify changes in the chemical composition of water as it flows through the aquifer.

The chloro-alkaline indices called CAI-I and CAI-II are calculated according to the relationships (2) and (3) where all ions are expressed in meq/l:

$$CAI - I = (Cl^- - (Na^+ + K^+))/(Cl^-) \qquad (2)$$
$$CAI - II = (Cl^- - (Na^+ + K^+))/(HCO_3^- + SO_4^{2-} + CO_3^{2-} + NO_3^-) \qquad (3)$$

When the indices are negative, the Ca^{2+} or Mg^{2+} cations of the groundwater are exchanged for the Na^+ or K^+ of the surrounding rock. Thus, the aquifer waters are enriched with Na^+ and K^+. On the other hand, if the chloroalkaline index values are positive, the opposite reaction occurs, i.e. the Na^+ or K^+ cations of the groundwater are exchanged for the Ca^{2+} or Mg^{2+} ions of the reservoir rock. As a result, groundwater is enriched with alkaline earth.

The Gibbs diagram is widely used in hydrogeological studies to identify the explanatory processes of water salinization. [33] recommends two diagrams to assess the dominant phenomenon between precipitation, weathering and evaporation in the geochemical evolution of groundwater.

The Gibbs diagrams represent the curve of the Na^+ / [Na^++ Ca^{2+}] and Cl^- / [Cl^- + HCO_3^-] ratios as a function of TDS. Diagrams are widely used to assess the functional source of dissolved chemical constituents.

- **Nitric Pollution**

The standard of potability required by the corresponding to the maximum permissible limit of 50 mg/l and the threshold of 13 mg/l [34], is used to evaluate the level of nitric pollution in samples, when, the correlation matrix is used to highlight the significant relationships at the probability threshold (0.05) between nitrate contents and the other parameters analyzed. The groundwater pollution was mapped using kriging to estimate the values of the nitrate in unsampled locations using the points around it. While, the average Cl/NO_3 ratio of 4.9 of river water is used as a reference point [35, 36], for estimating dnitrification effectiveness.A field survey is conducted on same water points covers type and use of fertilizers, type of crops grown and irrigation methods.

IV. RESULTS AND DISCUSSIONS

- **Groundwater Hydrochemistry**

The minimum and maximum pH values of groundwater vary between 6.7 and 10.5 respectively. These data reflect a pH ranging almost from neutral to strong alkalinity. The latter can be linked to high evaporation. The average pH value is 7.17 ± 0.52.

The electrical conductivity (EC) varies between 837 µS/cm and 3450 µS/cm with an average of 1565.94 µS/cm ± 424.62 µS/cm. This variation in EC data is due to the different geochemical processes that prevail in this field of study. TDS values range from 583 to 1407mg/l with an average of 835.61 ± 196.76mg/l. These values reflect relatively fresh and mineralized waters [37]. The total water hardness (HT), in $CaCO_3$ equivalent, ranges from 583 mg/l to 1407 mg/l with an average of 835.61 mg/l ± 196.76 mg/l. These results reflect relatively hard water [40]. Calcium (Ca^{2+}) concentrations vary between 26 mg/l and 135 mg/l and magnesium (Mg^{2+}) concentrations range between 0.7 mg/l and 74 mg/l. The average concentrations are respectively 60.16 mg/l ± 16.79 mg/l and 29.41 mg/l ± 18.18 mg/l. These values are related to the alluvial nature of the aquifer containing limestone fragments and the clay matrix responsible for the basic exchanges. The minimum sodium (Na^+) and potassium (K^+) contents vary between 60 mg/l and 0 mg/l respectively and the highest reach 300 mg/l and 19.5 mg/l respectively. The average Na^+ content is 128.05 mg/l ± 41.56 mg/l. The high Na^+ contents come from cationic exchanges with clays and sea spray from the Mediterranean Sea. Chloride (Cl^-) concentrations range from 15.60 mg/l to 66.30 mg/l and with an average of 34.53 mg/l ± 10.58 mg/l. Chlorides would probably come from marine sources through aerosols, as the geology has not revealed the existence of evaporative type salt rocks and the existence of marine intrusion. Chlorides may come from anthropogenic sources due to sewage discharges or livestock.

Sulphates (SO_4^{2-}) range from 78.8 mg/l to 501.40 mg/l (average of 212.21 mg/l ± 55.22 mg/l). These relatively high levels are related to a natural (gypsum, pyrite oxidation,) or anthropogenic (fertilizer, air pollution) presence. Bicarbonates (HCO_3^-) with an average of 321.54 mg/l ± 102.68 mg/l have values ranging from 153.5 mg/l to 793 mg/l. They result from carbonate weathering and the dissolution of carbonic acid in aquifers

The partial CO_2 pressures (pCO_2) of the groundwater in the alluvial aquifer range from -5.00 to -1.13 atm and have an average of -1.70 atm. This last value is much higher than the atmospheric reference set at - 3.5 atm, Table (1). Only one sample has data less than -3.5 atm. This high value suggests that groundwater is confined in a hydrogeological system open to CO_2 from the soil. Groundwater receives CO_2 from the respiration of the root system (rhizosphere) and the decomposition of the soil.

The Pearson correlation matrix in table (1), highlights the various chemical processes that occur in the aquifer between water and rock. These relationships are more or less complex. Among them, we will be able to link certain ionic associations (cation - anion). Ca^{2+} is correlated respectively to Cl^- (0.58), SO_4^{2-} (0.39) while Mg^{2+} is linked only to HCO_3^- with a value of 0.60. The correlations between Ca^{2+} and SO_4^{2-} on the one hand and Mg^{2+} and HCO_3^- on the other hand suggest the dissolution of gypsum and dolomite followed by the departure of Ca^{2+} and Mg^{2+} by base exchanges. Na^+ is significantly correlated to SO_4^{2-}, HCO_3^- and Cl^- with the values of (0.73), (0.57) and (0.55) respectively. The high correlation between Na^+ and SO_4^{2-} suggests the alteration of Glauber's salt (Na_2SO_4, $10H_2O$). The mean relationship between $Na+$ and Cl^- implies the phenomenon of halite dissolution. The EC of groundwater in the alluvial aquifer is controlled significantly in descending order by HCO_3^-, Ca^{2+}, Cl^-, SO_4^{2-} and Na^+. Summary statistics of the physical and chemical parameters of groundwater are provided in Table 1.

TABLE 1. Summary statistics of hydro chemical data for groundwater in the study area.

Parameters	Units	Minimum	maximum	Mean	Standard deviation
pH	-	6.74	10.50	7.17	0.52
EC	µS/cm	837	3450	1565.94	424.62
TDS	mg/l	583	1407	835.61	196.76
Ca^{2+}	mg/l	26.00	135.00	60.16	16.79
Mg^{2+}	mg/l	0.7	74	29.41	18.18
Na^+	mg/l	60.00	300.00	128.05	41.56
K^+	mg/l	0.00	19.50	2.58	3.60
Cl^-	mg/l	15.60	66.30	34.53	10.58

Parameters	Units	Minimum	maximum	Mean	Standard deviation
SO_4^{2-}	mg/l	78.80	501.40	212.21	55.22
HCO_3^-	mg/l	153.50	793.00	321.54	102.68
NO_3^-	mg/l	4.90	53.00	41.10	9.00
PO_4^{3-}	mg/l	0.00	1.914	0.073	0.277
HT ($CaCO_3$)	mg/l	150.26	491.72	270.99	81.37
pCO_2	atm.	-5.00	-1.13	-1.70	0.53
CAI-I	-	-9.00	-1.40	-5.00	1.50
CAI-II	-	-0.67	-0.24	-0.45	0.09

EC: electrical conductivity, HT: Total water hardness, pCO2: partial pressure, CAI-I, CAI-II: chloro-alkaline index, TDS: total dissolved solids.

According to correlation matrix (Table. 2), it is observed that NO_3^- is significantly correlated to Ca^{2+}, K^+ and PO_4^{3-} with respective values of 0.27, -0.62 and -0.47. The correlation between NO_3^- and Ca^{2+} is positive and relatively low compared to other significant coefficients. The relationship between NO_3^- and K^+ is negative and relatively high (-0.62). These two parameters evolve in an inversely proportional way. The mechanism for this behaviour is probably explained by the mobile nature of NO_3^- whereas K^+ is easily fixed in the clay-humic complex of the unsaturated zone. The correlation matrix revealed a negative and significant correlation coefficient between NO_3^- and PO_4^{3-} (-0.47). Phosphorus with low solubility in organic or inorganic particulate form binds to sediments (sources). The phosphate mineral fertilizer inputs, which would represent 58%, are much higher than other inputs, atmospheric, livestock manure and crop residues [38]. Phosphate is not as soluble as nitrate and ammonia and tends to adsorb to soil particles and enter water bodies through soil erosion [39].

TABLE 2. Correlation matrix.

Variables	pH	EC	Ca^{2+}	Mg^{2+}	Na^+	K^+	Cl^-	SO_4^{2-}	HCO_3^-	NO_3^-	PO_4^{3-}
pH	1										
EC	-0.061	1									
Ca^{2+}	-0.224	0.521	1								
Mg^{2+}	0.377	0.190	-0.131	1							
Na^+	0.030	0.787	0.314	0.167	1						
K^+	0.081	0.037	-0.220	0.068	0.168	1					
Cl^-	0.062	0.754	0.584	0.085	0.553	0.119	1				
SO_4^{2-}	-0.003	0.785	0.394	0.244	0.733	-0.020	0.547	1			
HCO_3^-	0.153	0.361	0.196	0.603	0.574	0.215	0.256	0.171	1		
NO_3^-	-0.055	0.052	0.275	-0.004	-0.099	-0.620	-0.199	0.186	-0.217	1	
PO_4^{3-}	0.197	0.097	-0.046	0.172	0.370	0.332	0.114	-0.043	0.541	-0.474	1

In bold, significant values, at probability threshold 0.05 (two-tailed test)

The representation of water points according to the Piper diagram shows that in the cation triangle, zone D (typical potassium sodium facies) is well represented followed by zone C (not dominant type). As for the triangle representing the anions, the large number of water points are in zone G (not dominant type) and very few samples in zones F (standard bicarbonate facies) and E (standard sulphate) (Fig. 3). In order of importance, the areas relating to the chemical facies encountered after projection of cations and anions are Na - Cl type with 52.7%, Mixed Ca - Mg - Cl type with 29.1%, Ca – HCO_3 type with 9.1% and Mixed Ca - Na – HCO_3 type with 9.1%.
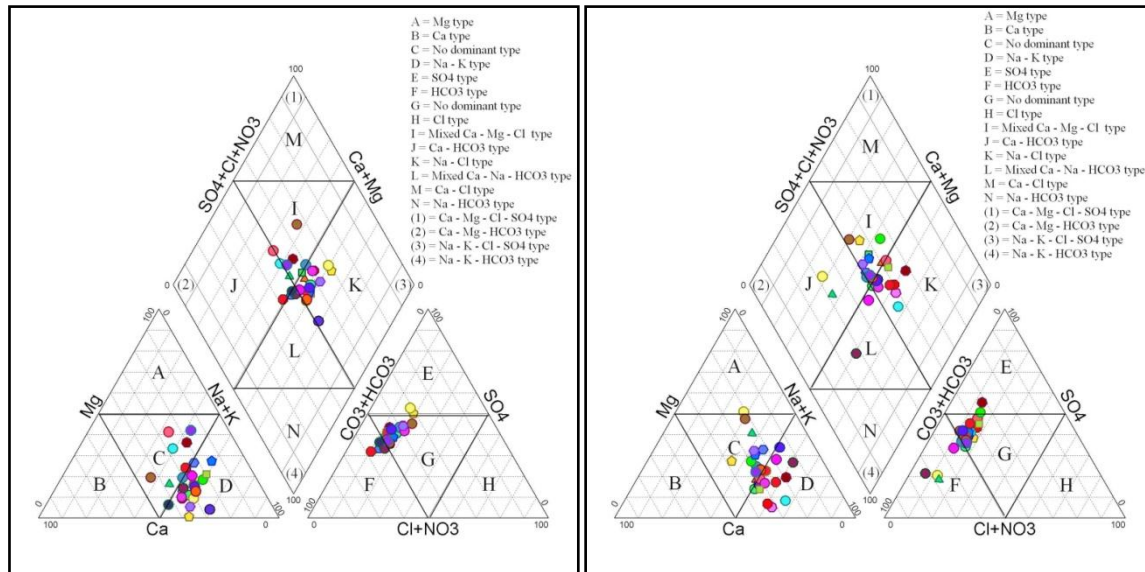
FIGURE 3. Groundwater facies according to the Piper diagram.

The chloro-alkaline indices (CAI-I and CAI-II) obtained in this study indicate all negative values. The minimum and maximum CAI-I and CAI-II data range from negative values and -1.40 and -0.67 and -0.24 respectively. The average values are -5.00 ±1.5 for CAI-I and -0.45±0.09 for CAI-II. In all indices, the values are below zero (table 1). These results underline that in the alluvial aquifer, cationic exchanges are carried out according to a single and unique reaction which consists in exchanging the Ca^{2+} and Mg^{2+} of the waters for the Na^+ and K^+ of the aquifer rock. As a result, groundwater is enriched with Na^+, K^+. The SI obtained show overall a single type of mineral that differs from the zero value (Fig. 4) On closer examination, we notice that carbonate minerals (calcite, dolomite and aragonite) are relatively close to the reference value (0) compared to other so-called evaporite minerals.
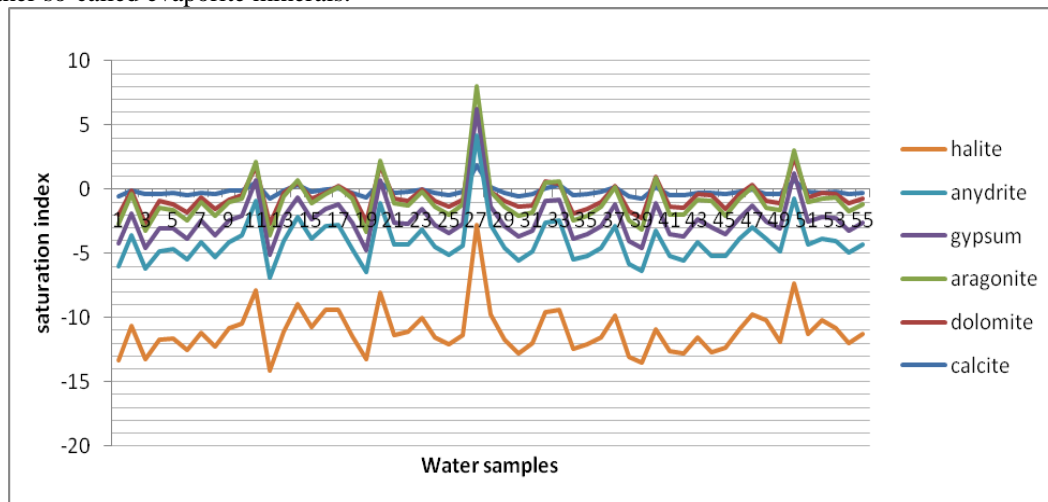

FIGURE 4. Groundwater saturation index .

The SI values of evaporite minerals show that anhydrite, gypsum and halite vary respectively between -2.23 and -1.33, between -2.01 and -1.11 and between -7.62 and -6.33 with respective averages of -1.71, -1.49 and -6.99 (Table. 3). These results clearly show that the groundwater of the Mitidja is in a state of under-saturation with respect to these minerals and therefore the possibilities of dissolution will be increased. On the other hand, carbonate minerals show that the IS of calcite, aragonite and dolomite range between -0.77 and 1.89, between -0.91 and 1.74 and between -2.32 and 4.39 with respective averages of -0.17; -0.31 and -0.39. These results suggest that these minerals are slightly under saturation for the majority of water points except for a few samples that indicate a tendency towards saturation. As a result, groundwater can still dissolve carbonate minerals and thus increase water mineralization.

	SI Calcite	SI Aragonite	SI Dolomite	SI Gypsum	SI Anhydrite	SI Halite
Minimum value	-0.77	-0.91	-2.32	-2.01	-2.23	-7.61
Maximum value	1.89	1.74	4.39	-1.11	-1.33	-6.33
Mean	-0.17	-0.31	-0.39	-1.49	-1.71	-6.99
Standard deviation	0.41	0.41	1.01	0.17	0.17	0.24

TABLE 3. Values of groundwater saturation indices.

The representation of the results of analyses of the water analysed according to the Gibbs diagram (Fig. 5) shows that only one major phenomenon is found in the evolution of the geochemical processes of the groundwater in the study area. Indeed, the points highlight the influence of rock weathering. From the diagram, we can see that the phenomenon of rock alteration is responsible for the current water chemistry. The alluvial plain and the Astian sandstones in hydraulic communication, are sedimentary rocks, easily degradable and altering in particular the clays. In addition, the relatively flat relief and high temperatures are parameters that favour the degradation of rocks by chemical means, particularly the exchange of bases. We also highlight the human action that through agricultural practices and domestic discharges in the absence of sanitation networks, in some places, contribute to the modification of groundwater chemistry. The results of the Gibbs diagram highlighted the importance of aquifer rock in geochemical groundwater processes. In order to better identify these mechanisms, we refer to some graphs widely used in the literature. A Na^+ / Cl^- ratio approximately equal to one is generally attributed to the dissolution of halite, while a ratio greater than one indicates that sodium is released by silicate alteration [40].
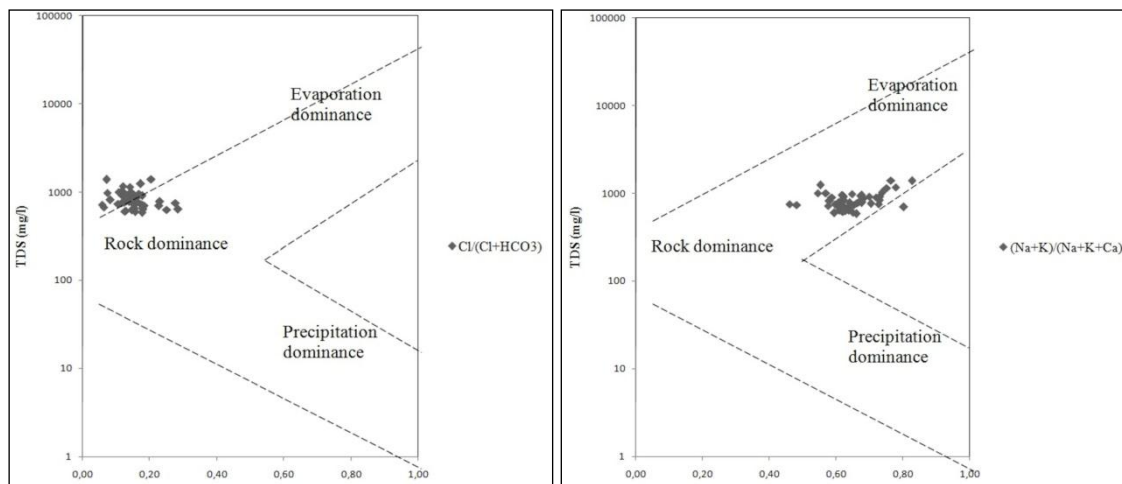
FIGURE 5. Gibbs diagram.

Dissolved ionic elements in groundwater are the product of weathering of rock minerals with a minor contribution from atmospheric precipitation and human activities. The contribution of atmospheric sources to dissolved salts in water bodies can be assessed by considering rainwater chemistry or by taking the ratios of elements to Cl^- [41]. The average ratios Na^+ / Cl^- and K^+ / Cl^- of the eastern Mitidja alluvial groundwater are 6.54 and 0.07 respectively. These ratios are higher than marine aerosols (Na^+ / Cl^- = 0.85 and K^+ / Cl^- = 0.0176) [43]. These results suggest that the contribution of atmospheric precipitations is limited in the region. The engine of chemical contribution is the one governed by the interaction of water with rock. This observation is confirmed by the Gibbs diagram (Fig.5).

- **Geochemical Processes Between Water and Solid Matrix**

The results of the Gibbs diagram highlighted the importance of aquifer rock in geochemical groundwater processes. In order to better identify these mechanisms, we refer to some graphs widely used in the literature.

A Na^+ / Cl^- ratio approximately equal to one is generally attributed to the dissolution of halite, while a ratio greater than one indicates that sodium is released by silicate alteration [42]. Figure 6, illustrates the relationship between Na^+ and Cl^-, the line represents the dilution line of seawater. The water samples show a clear enrichment in Na^+. As the water points are far from the seawater dilution line, we claim that the effect of the known salt bevel in the region did not affect the groundwater in the study area. These results corroborate the chloro alkaline indices that showed the passage of Na^+ and K^+ from the aquifer matrix to groundwater in exchange for Ca^{2+} and Mg^{2+}. Na ions would come from cationic exchanges, alteration of silicate minerals and probably pollution. The relationship between Na^+ and Cl^-, the line represents the dilution line of seawater. The water samples show a clear enrichment in Na^+. As the water points are far from the seawater dilution line, we claim that the effect of the known salt bevel in the region did not affect the groundwater in the study area. These results corroborate the

chloro alkaline indices that showed the passage of Na^+ and K^+ from the aquifer matrix to groundwater in exchange for Ca^{2+} and Mg^{2+}. Na ions would come from cationic exchanges, alteration of silicate minerals and probably pollution.

The representation of the water points studied according to the graphical $(Ca^{2+}+Mg^{2+})$ versus $(SO_4^{2-}+HCO_3^-)$ (fig. 9) highlights perfectly the positions with respect to the equiline line (1:1). Indeed, all the points are well below this reference line. Virtually no sample is aligned to the right or above it. The dominance of $SO_4^{2-}+HCO_3^-$ over $Ca^{2+}+Mg^{2+}$ is an indicator of silicate alteration. These graphical representations suggest that the main source of Ca^{2+}, Mg^{2+}, SO_4^{2-} and HCO_3^- in groundwater is away from the dissolution of carbonate (calcite, dolomite) and sulphate (gypsum, anhydrite) minerals but governed by silicate minerals.

The continuous supply of fertilizers to irrigated crops necessarily results in a source of NO_3^- which feeds the groundwater through soil leaching. This migration of NO_3^- to the aquifer can be facilitated by stormy rainfall events. Considering the average Cl/NO_3 ratio of 4.9 of river water, the majority of water points in the study area have $Cl/NO_3 < 4.9$ values meaning ineffective denitrification because NO_3^- accumulates in wells. Only four water points have ratio values above the reference showing effective denitrification in NO_3 reduction.

The results of the Gibbs diagram highlighted the importance of aquifer rock in geochemical groundwater processes. In order to better identify these mechanisms, we refer to some graphs widely used in the literature.

A Na^+ / Cl^- ratio approximately equal to one is generally attributed to the dissolution of halite, while a ratio greater than one indicates that sodium is released by silicate alteration.

The projection of the points underlines that the majority of the samples (Fig. 7 and Fig. 8) are located mainly in the silicate-altering zone. The alteration process of silicate minerals (feldspar), is accompanied by high concentrations of HCO_3^- [43].
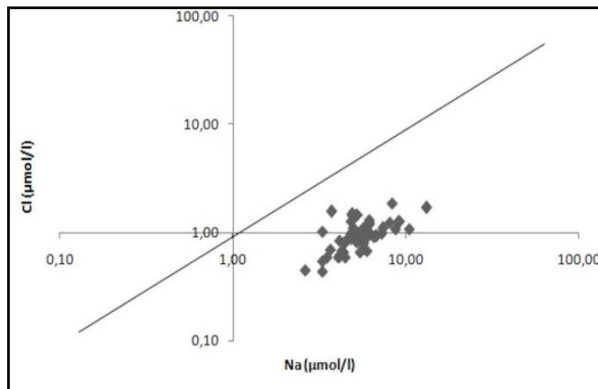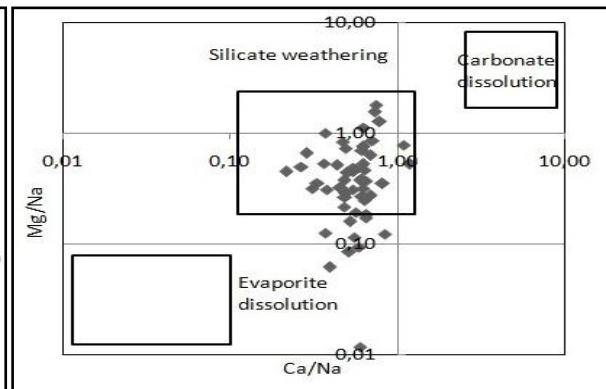

FIGURE 6. Cl^- versus Na^+

FIGURE 7. Mg^{2+}/Na^+ versus Ca^{2+}/Na^+
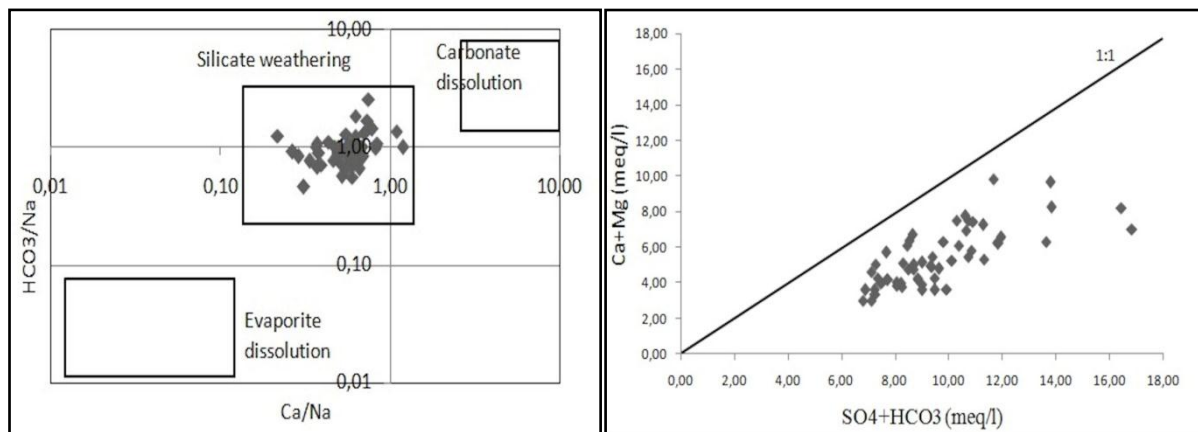
FIGURE 8. HCO_3^-/Na^+ versus Ca^{2+}/Na^+
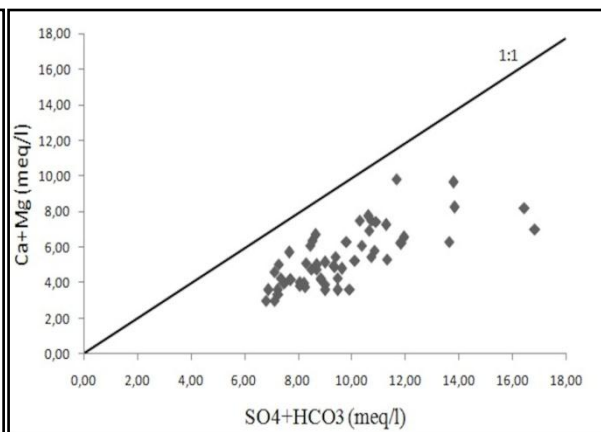
FIGURE 9. $(Ca^{2+}+Mg^{2+})$ versus $(SO_4^{2-} + HCO_3^-)$

The relatively high amounts of Na^+ and HCO_3^- can be explained by the presence of CO_2 in groundwater. We have already pointed out that almost all the samples studied have higher pCO_2 values than the atmospheric pCO_2. The plot of the pH versus log pCO_2 graph (fig. 10) shows that the pCO_2 values are negatively correlated with those of the pH. CO_2 partial pressure values decrease with increasing pH values [46]. This situation may be related to an aquifer where the residence time of the waters is relatively long. It is likely that the chemical reactions affecting the feldspar of the sandstone formations of the Astian are largely responsible for this chemical composition. The chemical reaction affecting feldspar is indicated by the relationship (4):
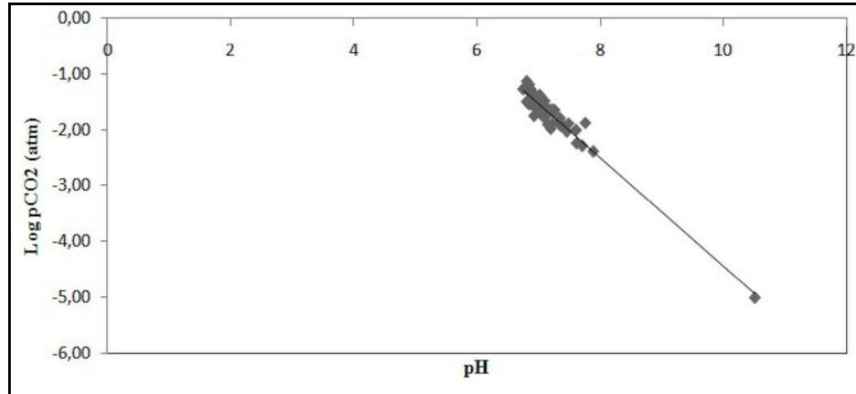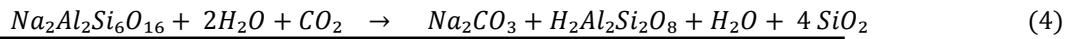
$$Na_2Al_2Si_6O_{16} + 2H_2O + CO_2 \rightarrow Na_2CO_3 + H_2Al_2Si_2O_8 + H_2O + 4\ SiO_2 \tag{4}$$

FIGURE 10. Relationship between pH and log (pCO_2).

- **Nitrate Contamination**

Agricultural activity often leads to deterioration in water quality caused by the massive use of fertilizers, pesticides and various chemicals. In comparison with the results, the minimum and maximum values of NO_3^- are 4.9 mg/l and 53 mg/l respectively. The arithmetic mean of the 55 samples is 48.1 mg/l $\pm$ 9 mg/l. The different values of the quartiles (1st, median, 3rd) are 40.2 mg/l, 42.9mg/l and 45.5mg/l. These results indicate a trend towards large values (Fig. 11) with a more or less homogeneous distribution. When comparing with the 50 mg/l standard recommended by the WHO for drinking water. Compared to the limit of 20 mg/l, considered as a low value, 3 water points (5.4%) have a lower value. On the other hand, 50 samples (91%) have NO_3^- contents ranging from 20 mg/l to 50 mg/l. Compared to the "human affected value" of 13 mg/l, about 95% of the points are contaminated. From these results, we can expect a general increase in NO_3^- levels, exceeding the standard of 50 mg/l, in groundwater, if measures are not taken in time to reduce this contamination.
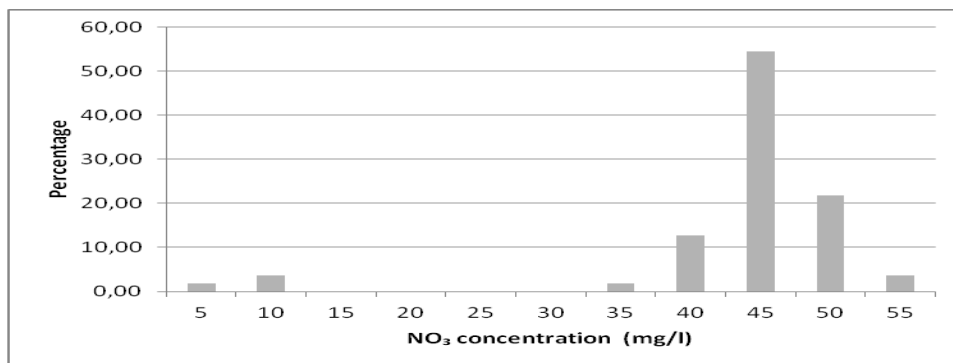

FIGURE 11. Distribution of NO_3^- in groundwater.

The nitrate concentration map (Fig. 12) shows values of NO_3^- exceeding 42 mg/l. Within this band, we observe well defined zonalities where NO_3^- concentrations are 44 mg/l or even higher. These localities are probably contaminated, not only by nitrogen fertilizers but also by domestic discharges because they are located near urban areas. Moreover, it is known that urban agriculture is often the cause of nitrogen pollution of groundwater from wastewater and solid waste discharges [44]. The rest of the study area is relatively less affected but nitrate levels remain well above the value of 40 mg/l, which is close to the 50 mg/l standard. These relatively high nitrate levels in groundwater are the result of the migration of these particles from fertilizer use to the groundwater table, due to rainwater leaching, especially with bare soils between crops [45]. The isovalent curves of NO_3^- contents are more or less closed in shape, indicating a rather localized or even punctual pollution. The curves do not correspond to the piezometry where the latter shows a flow towards the sea.
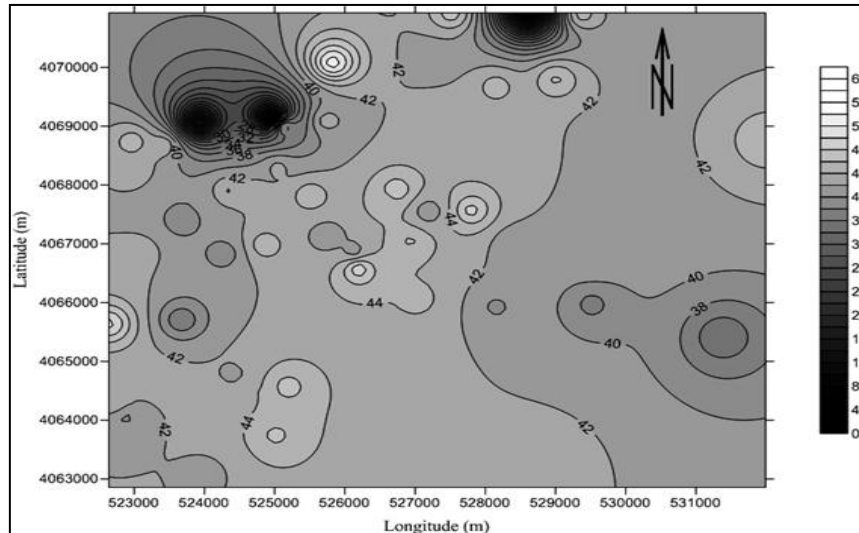
FIGURE 12. Spatial mapping of NO_3^- concentrations (mg/l).

CONCLUSIONS

The geochemical study of groundwater in the alluvial aquifer of the eastern Mitidja revealed fresh to mineralized waters with a relatively neutral pH. The waters are hard with dominant chemical facies of Na - Cl type (52.7%) and Mixed Ca - Mg - Cl type (29.1%). The hydrogeological system is open and exchanges take place between the soil and the aquifer. Chloro-alkaline indices indicate that the analyzed waters exchange Ca^{2+} and Mg^{2+} for Na^+ and K^+ from the aquifer rock. This result probably explains the dominance of the Na - Cl facies. Saturation indices suggest that, except for a few water points, carbonate minerals are in a slightly saturated situation while evaporite minerals are in saturation. As a result, waters can become more mineralized. The major geochemical process of groundwater, identified by the Gibbs diagram, is that related to rock weathering. The graphs and reports used showed that the majority of ions come from the alteration of silicate minerals present in the two communicating aquifers. The study of groundwater pollution by nitrates revealed the presence of concentrations with an abnormal tendency because the average is 48 mg/l. NO_3 contents between 20 mg/l and 50 mg/l represent 91% of the sampled points. With reference to the "human affected value", 95% of the water analysed is contaminated. The correlation matrix showed that NO_3 is significantly correlated with Ca, K and PO_4 in relation to fertilizers applied to crops. The hydro chemical dynamics between NO_3 on the one hand and K and PO_4 on the other is the opposite. The mapping of NO_3 concentrations has located the areas affected by the pollution. These are well defined, discontinuous and elongated bands in a generally north-south direction. Their location in urban areas and field surveys suggest that contamination by domestic discharges cannot be ruled out. With reference to the Cl/NO_3 ratio, denitrification is ineffective because NO_3 accumulates in wells. In order to reduce this pollution, raising farmers' awareness of water degradation from inputs is an urgent priority.

ACKNOWLEDGMENTS

REFERENCES

[1] Semar, A., Hartani, T., & Bachir, H. (2019). Soil and water salinity evaluation in new agriculture land under arid climate, the case of the Hassi Miloud area, Algeria. *Euro-Mediterranean Journal for Environmental Integration*, *4*(1), 1-14.

[2] Semar, A., Bachir, H., & Bourafai, S. (2021). Hydrochemical characteristics of aquifers and their predicted impact on soil properties in Biskra region, Algeria. *Egyptian Journal of Agricultural Research*, *99,* (2), 205-220.

[3] Brahim, F. B., Boughariou, E., & Bouri, S. (2021). Multicriteria-analysis of deep groundwater quality using WQI and fuzzy logic tool in GIS: A case study of Kebilli region, SW Tunisia. Journal of African Earth Sciences, 180, 104224.

[3] Moya, C. E., Raiber, M., Taulis, M., Taulis, M., and Cox, M.E. (2015). Hydrochemical evolution and groundwater flow processes in the Galilee and Eromanga basins, Great Artesian Basin, Australia: A multivariate statistical approach. Total environnement science. Volume 508, 411-426.

Page 10

[4] Villegas, P., Paredes, V., Betancur T. and Ribeiro L. (2013). Assessing the hydrochemistry of the Urabá Aquifer, Colombia by principal component analysis. Journal of Geochemical Exploration, 134, 120-129.

[5] Ravikumar P., R. K. Somashekar R. K., and Mhasizonuo A. (2011). Hydrochemistry and evaluation of groundwater suitability for irrigation and drinking in the the Markandeya river basin, Belgaum District, Karnataka State, India. Environmental Monitorig and assessment, Volume 173, 1, 459-487.

[6] Prasanna, M.V., Chidambaram, S., Senthil, Kumar, G., Ramanathan, A.L. and Nainwal, H.C. (2010). Hydrogeochemical Assessment of Groundwater in Neyveli Basin, Cuddalore District, South India. Arabian Journal of Geosciences. 4, 1-2, 319-330.

[7] Psychoyou, M., Mimides, T., Rizos, S., and Sgoubopoulou, A. (2007). Groundwater hydrochemistry at Balkan coastal plains, the case of Marathon of Attica, Greece. Dessalement, 213, 230-237.

[8] Subyani, A.M. (2005). Hydrochemical identification and salinity problem of ground water in Wadi Yalamlam basin, Western Saudi Arabia. Journal of Arid Environments 60. 53-66.

[9] Wick, K., Heumesser, C., and Schmid, E. (2012). Groundwater nitrate contamination: factors and indicators. Journal of environmental management, 111, 178-186.

[10] Rivett, M. O., Buss, S. R., Morgan, P., Smith, J. W., and Bemment, C. D. (2008). Nitrate attenuation in groundwater: a review of biogeochemical controlling processes. Water research, 42, 16, 4215-4232.

[11] Mahvi, A. H., Nouri, J., Babaei, A. A., & Nabizadeh, R. (2005). Agricultural activities impact on groundwater nitrate pollution. International Journal of Environmental Science & Technology, *2*, 1, 41-47.

[12] Maynard, D. N., Barker, A. V., Minotti, P. L., & Peck, N. H. (1976). Nitrate accumulation in vegetables. *Advances in Agronomy*, *28*, 71-118.

[13] Meddi, M., Boufekane, A., & Meddi, H. (2015). *Recharge artificielle de la nappe de la Mitidja*. Éditions universitaires européennes.

[14] Trigo, R., Xoplaki, E., Zorita, E., Luterbacher, J., Krichak, S. Alpert, P., Jacobeit, J., Sáenz, J., Fernández, J, González-Rouco, F., Garcia-Herrera, R., Rodo, X., Brunetti, M., Nanni, T., Maugeri, M., Türke, M., Gimeno, L., Ribera, P., Brunet, M., Trigo, I., Crepon, M., Mariotti, A. (2006). Relations between variability in the Mediterranean region and mid-latitude variability.Developments in Earth and Environmental Sciences, 4,179-226.

[15] Hartani, T., Imache, A., Kuper, M., & Bouarfa, S. (2011). La Mitidja vingt ans après : Réalités agricoles aux portes d'Alger. Editions Quae, p 290.

[16] Lagoun, A.M., Bouzid-Lagha, S., Bendjaballah-Lalaoui N., Saibi, H., (2021). Geographic information system–based approach and statistical modeling for assessing nitrate distribution in the Mitidja aquifer, Northern Algeria. Environmental Monitoring and Assessment, 10, P 193(10).

[17] Zamiche S, Hamaidi-Chergui F, Demiai A.Pollution of the quaternary aquifer of mitidja (Algeria) by nitrates: origins and impacts on the quality of water for human consumption. J. Fundam. Appl. Sci., 2018, 10(1), 113-131

[18] Saida, S, Tarik H, Abdellah A, Farid H, Hakim B. (2017). Assessment of Groundwater Vulnerability to Nitrate Based on the Optimised DRASTIC Models in the GIS Environment (Case of Sidi Rached Basin, Algeria). *Geosciences*. 7(2): 20.

[19] Mimouni, O., Cheikh Lounis, G., Kabouche, S., & Menceur, H. (2015). Vulnerability to pollution of mitidja palin alluvial aquifer (Algiers-Algeria). *Int. J. Enhanced Res. Sci. Technol. Engineering*, 137-143.

[20] Khous, D., Ait-amar, H., Belaidi, M. and Chorfi H. (2019). Geochemical and isotopic assessment of the groundwater quality in the alluvial aquifer of the Eastern Mitidja plain. Water ressources. 46,443.

[21] Glangeaud, L., Aymé, A., Caire, A., Mattauer, M., & Muraour, P. (1952). Geological history of the province of Algiers. XIX cong. Geol. Inter. Monogr. Algeria Region, 1st series, (25).

[22] Meghraoui M. (1991). System of blind reversed faults associated with the Chenoua Mont Tipasa earthquake of October 29, 1989 (Center-North Algeria).Terra Nova, 3, 84-93.

[23] Boudiaf, A. (1996). Etude sismotectonique de la région d'Alger et de la Kabylie (Algérie): utilisation des modèles numériques de terrains (MNT) et de la télédétection pour la reconnaissance des structures tectoniques actives: contribution à l'évaluation de l'aléa sismique (Doctoral dissertation, Montpellier 2).

[24] Sekkal, R. (1986). Hydrologie de la nappe de la Mitidja (Algérie): étude hydrodynamique des champs captants de la ville d'Alger (Doctoral dissertation, Université Scientifique et Médicale de Grenoble).

[25] Queney P. (1937). Le régime pluviométrique de l'Algérie et son évolutiondepuis 1850. Météorologie 427-440

[26] Queney, P. (1943) .Les fronts atmosphériques permanents et leurs pertur-bations. (Travaux de l'Institut de Météorologie, fasc. 3. Alger. 1-6

[27] Rodier J., 2009. Analysis of water, 9th edition. Dunod, Paris, 1526.

[28] Domenico, P. A., and Schwartz, F. W. (1998). Physical and chemical hydrogeology (Vol. 506). New York: Wiley.

[29] Simler, R. (2007) Diagrammes. Laboratoire d'hydrogéologie. Université d'Avignon, Logiciel d'hydrochimie multilangage en distribution libre. France

[30] Appelo, C.A.J. and Postma, D. (1999). Chemical analysis of groundwater, Geochemistry, groundwater and pollution. Rotterdam, Balkema.

[31] Drever, J.I. (1997) The geochemistry of natural waters. Prentice-Hall, Englewood Cliffs, 436.

[32] Schoeller, (1965). Qualitative Evaluation of Groundwater Resources. In Methods and Techniques of Groundwater Investigations and Developments. UNESCO

[33] Gibbs, R. J. (1970). Mechanisms Controlling World's Water Chemistry. Science, 170, 3962, 1088- 1090.

[34] Burkart, M.R, Kolpin, D.W. (1993). Hydrologic and land use factors associated with herbicides and nitrates in near-surface aquifers. Journal of Environmental Quality, 22, 646-656.

[35] Majumder, R.K., Hasnat, M.A., Hossain, S., Ikeue, K., and Machida, M. (2008). An exploration of nitrate concentrations in groundwater aquifers of central-west region of Bangladesh. Journal of Hazardous Materials, 159, 536-543

[36] Raju, N. J., Patel, P., Gurung, D., Ram, P., Gossel, W., & Wycisk, P. (2015). Geochemical assessment of groundwater quality in the Dun valley of central Nepal using chemometric method and geochemical modeling. Groundwater for Sustainable Development, 1(1-2), 135-145.

[37] Sarin, M. M. Krishnaswamy S., Dilli. K., Somayajulu. B.L.K and Moore, W.S. (1989). Major ion chemistry of the Ganga-Brahmaputra river system: weathering processes and fluxes to the Bay of Bengal. *Geochim. Cosmochim. Acta*, *53*, 997-1009.

[38] Kundu, M.C. and Mandal, B. (2009). Agricultural Activities Influence Nitrate and Fluoride Contamination in Drinking Groundwater of an Intensively Cultivated District in India. Water, Air, and Soil Pollution, 198, 1-4, 243-252.

[39] Evans, A. E., Mateo-Sagasta, J., Qadir, M., Boelee, E., & Ippolito, A. (2019). Agricultural water pollution: key knowledge gaps and research needs. Current opinion in environmental sustainability, 36, 20-27.

[40] He, S., & Wu, J. (2019). Hydrogeochemical characteristics, groundwater quality, and health risks from hexavalent chromium and nitrate in groundwater of Huanhe Formation in Wuqi county, northwest China. Exposure and Health, 11(2), 125-137.

[41] Liu, F., Song, X., Yang, L., Zhang, Y., Han, D., Ma, Y., and Bu, H. (2015), Identifying the origin and geochemical evolution of groundwater using hydrochemistry and stable isotopes in the Subei Lake basin,Ordos energy base, Northwestern China. Hydrology and Earth System Science,19, 551-565.

[42] Talib, M.A., Tang, Z., Shahab, A., Siddique, J., Faheem, M. and Fatima, M. (2019). Hydrogeochemical Characterization and Suitability Assessment of Groundwater: A Case Study in Central Sindh, Pakistan. International journal of environmental research and public health, 16 (5), 886.

[43] Zhang, Y., Li, F., Zhang, Q., Li, J., & Liu, Q. (2014). Tracing Nitrate Pollution Sources and Transformation in Surfaceand Ground-Waters Using Environmental Isotopes Science of the Total Environment, 490, 213-222.

[44] Wakida, F.N. and Lerner, D.N., 2005. Non-agricultural sources of groundwater nitrate: a review and case study. Water research, 39, 1, 3-16.

[45] Rodriguez-Galiano, V. F., Luque-Espinar, J. A., Chica-Olmo, M., & Mendes, M. P. (2018). Feature selection approaches for predictive modelling of groundwater nitrate pollution: An evaluation of flters, embedded and wrapper methods. Science of the total environment, 624, 661-672.